Biophysical Chemistry 156 (2011) 140–145

Contents lists available at ScienceDirect

Biophysical Chemistry

journal homepage: http://www.elsevier.com/locate/biophyschem

Salt bridges in prion proteins are necessary for high-affinity binding to the monoclonal antibody T2

Eriko Sasamori [a], Mieko Kato [a,b], Kosuke Maki [c], Yuichi Tagawa [d], Yoshiro Hanyu [a,*]

[a] Molecular Composite Medicine Research Group, Biomedical Research Institute, National Institute of Advanced Industrial Science and Technology, 1-1-1 Higashi, Tsukuba-shi, Ibaraki, Japan
[b] Graduate School of Life and Environmental Sciences, University of Tsukuba, 1-1-1 Tennoudai, Tsukuba-shi, Ibaraki, Japan
[c] Department of Physics, Graduate School of Sciences, Nagoya University, Furo-cho, Chikusa-ku, Nagoya-shi, Aichi, Japan
[d] Research Team for Bacterial/Parasitic Diseases, National Institute of Animal Health, 3-1-5 Kannondai, Tsukuba-shi, Ibaraki, Japan

ARTICLE INFO

Article history:
Received 22 January 2011
Received in revised form 31 March 2011
Accepted 31 March 2011
Available online 8 April 2011

Keywords:
Prion protein
Salt bridges
Mutation
Conformation
Interaction
Antibody

ABSTRACT

We studied the role of the 2 salt bridges (Asp143–Arg147 and Asp146–Arg150) in helix 1 of mouse prion protein (PrP) on the formation of the complex between PrP and the monoclonal antibody T2. We introduced 6 charge-changing mutations to the amino acid residues associated with the salt bridges. Analysis of the circular dichroism spectra of the mutant PrPs showed that the salt bridge mutations did not change the secondary structures. We analyzed the kinetics of the association and dissociation of the PrPs with the T2 antibody. The results showed that the association kinetics were not significantly different among the variants except Arg150Lys, while the dissociation rate of the neutralized-charge variants was 2 orders of magnitude higher than that of the wild type. These results indicate that salt bridges make the interaction of PrP with T2 tighter by slowing down dissociation.

1. Introduction

Creutzfeldt–Jakob disease and Gerstmann–Sträussler–Sheinker disease in humans, bovine spongiform encephalopathy (BSE) in cattle, and scrapie in sheep and goats are lethal neurodegenerative illnesses [1,2]. All of these are prion diseases, and the main pathogenic factor involved in their development is considered to be an abnormal prion protein (PrP^{Sc}) generated by posttranslational modification of the host-encoded cellular prion protein PrP^{C} [3]. Although the mechanism of conversion from PrP^{C} to PrP^{Sc} has not been elucidated in detail, the conversion is known to be initiated by the contact of PrP^{C} with exogenous PrP^{Sc}. Diagnosis of prion diseases has thus far been carried out by immunohistochemical examination [4,5] and western blotting [6] to detect accumulated PrP^{Sc}. Various antibodies have been prepared and used for diagnosis and epidemiologic surveillance of prion protein diseases. Some anti-PrP^{C} antibodies can inhibit the conversion of PrP^{C} to PrP^{Sc} and the accumulation of PrP^{Sc} by interfering with the association of PrP^{C} with PrP^{Sc} [7–11]. Investigation of the mechanisms by which the antibodies recognize the prion proteins will be helpful for elucidating the mechanism underlying the conversion of PrP^{C} to PrP^{Sc}.

The anti-PrP monoclonal antibody T2 was developed from PrP-knockout mice immunized with recombinant mouse PrP120–230. This antibody has been used to detect BSE in Japan because it shows strong cross-reactivity with human and bovine PrPs [6]. Additionally, it was reported that the T2 antibody inhibits PrP^{Sc} accumulation in cultured cells [12]. Recently, we reported that this antibody recognized both a disulfide bond and salt bridges in PrP [13]. Nuclear magnetic resonance (NMR) analysis has revealed that the recombinant mouse PrP fragment PrP120–230 consists of 2 short β-strands (strand 1, 126–129 and strand 2, 159–162) and 3 α-helices (helix 1, 142–152; helix 2, 177–191; and helix 3, 198–215) [14]. The chemical bonds, a disulfide bond (Cys178–Cys213) and 2 salt bridges (Asp143–Arg147 and Asp146–Arg150), are important in maintaining the tertiary structure of PrP. For example, the disulfide bond connects helix 2 to helix 3. The conversion of PrP^{C} to PrP^{Sc} was found to be inhibited by reduction and alkylation treatment of the disulfide bond in a cell-free conversion system [15]. The salt bridges contribute to the stability of the helix more than the typical salt bridges found in most proteins. Helix 1 consists mainly of hydrophilic residues (DWEDRYYRENM) without hydrophobic contacts with other protein

Abbreviations: BSE, bovine spongiform encephalopathy; CD, circular dichroism; k_a, association rate constant; k_d, dissociation rate constant; K_D, dissociation constant; PAGE, polyacrylamide gel electrophoresis; PrP, prion protein; PrP^{C}, cellular prion protein; PrP^{Sc}, abnormal prion protein; PVDF, polyvinylidene difluoride; SDS, sodium dodecyl sulfate.

* Corresponding author at: Molecular Composite Medicine Research Group, Biomedical Research Institute, National Institute of Advanced Industrial Science and Technology, 1-1-1 Higashi, Tsukuba-shi, Ibaraki 305-8566, Japan. Tel.: +81 29 861 2732; fax: +81 29 861 2740.
E-mail address: y.hanyu@aist.go.jp (Y. Hanyu).

0301-4622/$ – see front matter © 2011 Elsevier B.V. All rights reserved.
doi:10.1016/j.bpc.2011.03.011

regions. Without forming hydrophobic contacts with the protein core for stabilization, helix 1 is stabilized by the 2 internal salt bridges [16]. Molecular dynamics simulations have shown that a double mutant (mouse PrP: D146A and R150A) with alterations that affect the second salt bridge has increased conformational fluctuations [17]. In addition, it has been shown that the introduction of mutations to the salt bridges inhibits the conversion of PrP^{C} to PrP^{Sc} in a cell-free conversion system [18]. Our previous experiments have revealed that 4 mutations (C178M, C213M, D146N, and R150H) reduced PrP reactivity with the T2 antibody compared to wild-type PrP; in particular, the salt bridge mutants D146N and R150H were found to have almost completely lost reactivity to the T2 antibody [13]. Most specific antibodies, which inhibit the conversion and accumulation of PrP^{Sc}, interact with the helix 1 region of PrP^{C} [7–11], which is the case for the T2 antibody [13]. Therefore, characterizing the mechanisms by which the T2 antibody recognizes the salt bridges will provide an insight into the PrP^{C}-to-PrP^{Sc} conversion mechanism. We introduced mutations into the 4 residues that make up the 2 salt bridges (Asp143–Arg147 and Asp146–Arg150) and produced 6 mutants. In 4 of the 6 mutants, the aspartic acid and arginine were replaced with asparagine and histidine, respectively, to significantly reduce the charge (neutralized-charge variants: D143N, D146N, R147H, and R150H), while in the other 2 mutants, the aspartic acid and arginine were replaced with glutamate and lysine, respectively, (like-charge variants: D146E and R150K). We evaluated the secondary structure of the 6 mutants via circular dichroism (CD) studies. In addition, we analyzed the kinetics of the association and dissociation of the PrP fragment and its variants with the T2 antibody to examine the specific binding mechanisms. We found that the salt bridges in helix 1 affect the dissociation kinetics and dominate the affinity of the PrP fragment to the T2 antibody.

2. Material and methods

2.1. Antibody

The anti-PrP monoclonal antibody T2, which was used in all the experiments, was provided by Dr. T. Yokoyama of the National Institute of Animal Health (NIAH, Japan).

2.2. Expression of recombinant PrPs

The amino acid sequence used was based on that of mouse PrP. DNA for the wild-type fragment and PrP120–230 salt bridge mutants was synthesized by GenScript (NJ, USA), digested with *Eco*RI and *Xho*I restriction enzymes, and inserted into the pET22b(+) vector for periplasmic protein expression. After the nucleotide sequences were confirmed, the resulting expression plasmids were transformed in *Escherichia coli* BL21 (DE3) (Novagen, CA, USA). The transformants were cultured at 37 °C in 250 mL Luria–Bertani (LB) medium containing 50 μg/mL of ampicillin until an A_{595} of 0.4 was reached. The cells were then incubated at 25 °C for an additional 6 h in the presence of 0.1 mM isopropyl-β-D(−)-thiogalactopyranoside and pelleted by centrifugation.

2.3. Purification of recombinant PrPs from periplasmic extracts

The pelleted cells that expressed the wild-type fragment and His-tagged PrP120–230 salt bridge mutants were suspended in resuspension buffer (30 mM Tris–HCl, 20% sucrose). EDTA was added at a final concentration of 1.0 mM, and the suspension was rotated at 4 °C for 10 min. The cell lysates were centrifuged at 8000×*g* at 4 °C for 10 min. The pellets were collected, resuspended in 5 mM $MgSO_4$, rotated at 4 °C for 10 min, and centrifuged at 8000×*g* at 4 °C for 20 min. The periplasmic supernatants were collected and diluted with binding buffer (20 mM phosphate, 0.5 M NaCl, and 20 mM imidazole [pH 7.6]). The diluents were filtered through a 0.22-μm filter and loaded onto a 1-mL HisTrap-FF column (GE Healthcare, MA, USA) that was equilibrated with binding buffer. The His-tagged fragments were eluted with a linear gradient of 20–500 mM imidazole in binding buffer. The purified PrP fragments were dialyzed against phosphate-buffered saline (PBS) (pH 7.4) and stored at −30 °C. The purified PrP fragments were dissolved in sample buffer (2% sodium dodecyl sulfate [SDS], 5% 2-mercaptoethanol, 10% glycerol, 0.01% bromophenol blue, 62.5 mM Tris–HCl [pH 6.8]) and boiled at 95 °C for 5 min. The samples were separated by SDS-polyacrylamide gel electrophoresis (SDS-PAGE) in a denaturing running buffer (containing 0.1% SDS). The gel was stained with coomassie brilliant blue (Bio-safe Coomassie; Bio-Rad Laboratories, CA, USA) or transferred by electrophoresis to polyvinylidene difluoride (PVDF) membranes using a transfer buffer (without SDS). The blots were blocked in PBST (PBS with 0.05% Tween 20) containing 5% nonfat dry milk. After they were washed with PBST, the blots were incubated with the T2 antibody for 2 h and washed with PBST. Subsequently, they were incubated with anti-mouse IgG antibody conjugated to horseradish peroxidase for 1 h, washed with PBST, and developed using a chemiluminescent HRP substrate kit (Immobilon Western; Millipore, MA, USA), and the chemiluminescence signal was detected using Chemi-Stage CC16mini (KURABO, Osaka, Japan).

2.4. CD spectroscopy

CD spectroscopy was performed using a J820 CD spectropolarimeter (JASCO, Tokyo, Japan) in a 0.1-cm cuvette for far-UV CD spectra. Spectra were measured at protein concentrations of 0.1–0.25 mg/mL in PBS (pH 7.4) at 25 °C. The spectra were scanned from 200 nm to 250 nm 4 times with a 0.2-nm scanning interval and were corrected for the buffer.

2.5. Kinetic analysis by surface plasmon resonance

Kinetic analysis was performed using a Biacore J system (GE Healthcare, MA, USA). The T2 antibody was amine coupled to the CM5 sensor chip as instructed by the manufacturer (NHS/EDC coupling kit, GE Healthcare). Wild-type PrP120–230 and its salt bridge mutants were dissolved in HBS-EP buffer (0.01 M HEPES [pH 7.4], 0.15 M NaCl, 3 mM EDTA, and 0.005% surfactant P20) and injected as the analyte solution. All measurements were performed at a flow rate of 30 μL/min at 25 °C, and the interaction surface was regenerated with glycine-HCl (pH 1.5). Data were evaluated using the Biaevaluation software (version 4.1; GE Healthcare).

3. Results

3.1. Affinity of PrP120–230 salt bridge mutants to the T2 antibody as determined by western blot analysis

The T2 antibody recognizes 2 contiguous regions of the PrP120–230 fragment located far apart from each other along the primary structure, indicating that the antibody recognizes the tertiary structure of PrP120–230 [13]. Helix 1 of mouse PrP is located in 1 of these recognition regions, which has 2 salt bridges (Asp143–Arg147 and Asp146–Arg150) [14]. In our previous study, we reported that the mutations introduced into Asp146 and Arg150 decrease the reactivity of the resultant protein with the T2 antibody [13]. To systematically analyze the influence of these 2 salt bridges on the recognition of the PrP120–230 fragment by the T2 antibody, we introduced mutations into the 2 salt bridge residues (Asp143–Arg147 and Asp146–Arg150) to change their charges to be neutral or significantly reduced (Fig. 1(a)). The amino acids of the first salt bridge, Asp143 and Arg147, were replaced with residues with a neutral charge (Asp to Asn or Arg to His), and the amino acids of the second salt bridge, Asp146 and Arg150, were replaced with neutrally (Asp to Asn or Arg to His) or similarly charged residues (Asp to Glu or Arg to Lys). The periplasmic extract of the recombinant proteins was

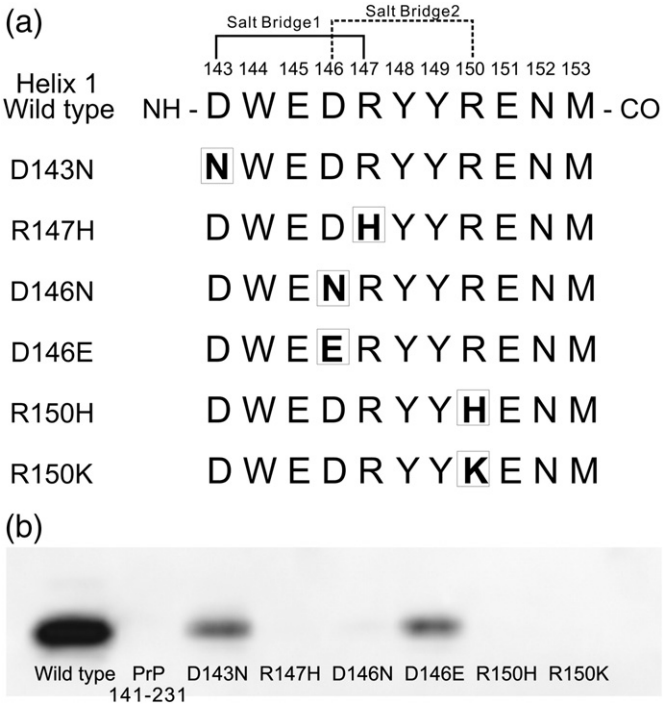

Fig. 1. Preparation and western blot analysis of salt bridge mutants. The amino acid sequence used was based on that of mouse PrP. (a) PrP constructs were made with mutations in the residues proposed to be involved in the 2 salt bridges in helix 1. For salt bridge 1, only mutants with a neutral charge were prepared. For salt bridge 2, mutants with a neutral charge and those with a similar charge were prepared. (b) Western blot analysis with the T2 antibody. The same amount of purified proteins was analyzed with the T2 antibody. Wild-type PrP is PrP120–230, which was used as the positive control. PrP141–231 was the negative control.

purified by affinity chromatography, dialyzed against PBS, and stored at −30 °C. We used western blotting to examine whether the T2 antibody would recognize PrP recombinants (Fig. 1(b)). Wild-type PrP120–230 was used as the positive control (lane 1). PrP141–231, which had no reactivity with the T2 antibody, was used as the negative control (lane 2).

The T2 antibody recognized only D143N from among the 4 neutralized-charge mutants (D143N, D146N, R147H and R150H). On the other hand, for the like-charge mutants, T2 recognized D146E but did not completely recognize R150K. T2 reactivity to D143N and D146E was decreased compared to that to the wild-type protein. Mutations that break the salt bridges decrease the reactivity of T2 toward PrP. However, there are some exceptions to this trend, such as the like-charge mutant R150K and the neutralized charge mutant D143N. The mutations introduced to break the salt bridges actually not only induced the breakdown of the salt bridges but also had other effects on PrP. Further, the contributions of each salt bridge to the interaction with the T2 antibody are not identical. To further study the effects of the mutations, we kinetically investigated the interactions.

3.2. CD spectroscopy of the wild-type and salt bridge mutants of PrP120–230

We measured the CD spectra in the far-UV region to evaluate the effects of the 6 mutations on the secondary structure of the PrP120–230 fragment (Fig. 2). All the spectra of the 6 salt bridge mutants were qualitatively similar to those of the wild-type PrP120–230, indicating that the secondary structure of PrP was not greatly influenced by the mutations introduced in the salt bridges in helix 1. At measurement, the concentration of R150H was lower than that of the other proteins, because of which its spectrum was slightly disordered than that of the rest. The spectra of the 2 like-charge mutants (D146E and R150K) were almost identical to those of the wild-type fragment, all of which showed 2 negative peaks at 208 and 222 nm reflecting an α-helical structure (Fig. 2). On the other hand, the ellipticity values of the 4 neutralized-charge mutants (D143N, R147H, D146N, and R150H) were slightly lower than the value of the wild-type fragment, suggesting that the α-helical structure is disturbed by these mutations.

3.3. Kinetic analysis of the association and dissociation of wild-type PrP120–230 and its salt bridge mutants with the T2 antibody

We analyzed the kinetics of the association and dissociation of the wild-type fragment and the salt bridge mutants with the T2 antibody (Fig. 3). The T2 antibody was immobilized onto a CM5 sensor tip by using the standard EDC/NHS ammine-coupling method, and the PrP fragments were injected into a Biacore J system at various concentrations. All the Biacore kinetic experiments were conducted at 25 °C. All the sensorgrams were fitted to a mass transfer-limiting model, and the rate constants for the association and dissociation kinetics were calculated. Wild-type PrP120–230 showed strong reactivity toward the T2 antibody (Fig. 3(a)). The association (k_a) and dissociation (k_d) rate constants as well as the dissociation constants (K_D) are shown in Table 1. The k_a and k_d values of the wild-type fragment calculated by curve fitting were $55.63 \pm 4.92 \times 10^4\ M^{-1}\ s^{-1}$ and $0.24 \pm 0.02 \times 10^{-3}\ s^{-1}$, respectively. The K_D value of the wild-type fragment was $4.41 \pm 0.70 \times 10^{-10}$ M (Table 1). The PrP141–231 fragment, the negative control, appeared virtually unbound to the T2 antibody (Fig. 3(b)). The k_a values of D143N, R147H, D146N, and D146E were similar to the value of the wild-type fragment. However, the k_a values of R150H ($8.13 \pm 0.71 \times 10^4\ M^{-1}\ s^{-1}$) and R150K ($0.27 \pm 0.02 \times 10^4\ M^{-1}\ s^{-1}$) were less than the value of the wild-type fragment. In contrast, the k_d values of the mutants were greater than the value of the wild-type fragment, except for D143N, whose value was almost the same as that of the wild-type fragment. The k_d values varied on the basis of the change in the charge because of the mutations in the salt bridges. The association kinetics did not differ significantly among the variants except Arg150Lys, while the dissociation rate of the like-charge and neutralized-charge variants were 1 and 2 orders of magnitude higher, respectively, compared to the wild type.

4. Discussion

4.1. Preparation of salt bridge mutants and reactivity toward the T2 antibody

We used western blotting to examine whether the T2 antibody recognized recombinant PrP mutants (Fig. 1(b)). Although T2 recognized D143N and D146E, the reactivity of both mutants was diminished compared with that of the wild-type fragment. In contrast, T2 did not recognize the D146N, R147H, R150H, and R150K mutants. The mutations introduced into the aspartic acid residues led to decreased reactivity with T2, except in the case of the D146N mutation. Further, the mutant with changes to the arginine residue showed no reactivity with the T2 antibody. Thus, the reactivity differed depending on the kind of amino acid introduced. Norstrom and Mastrianni reported a correlation between the formation of a salt bridge and the ability to convert PrP^C to PrP^{Sc} [18]. They created like-charge mutants, neutralized-charge mutants, and reverse-charge mutants for the salt bridge residues of PrP. Using a cell-free conversion system, they tested whether their mutants had the abilities of conversion and proteinase K resistance. They found that both the like-charge and neutralized charge mutants of aspartic acid permit conversion, while both mutants of arginine do not permit conversion or permit decreased conversion. Our western blot analysis of the reactivity between salt bridge mutants and T2 shows similar results. Salt bridge mutants that could convert were recognized by T2 to the same extent as the wild-type fragment; however, those that could not convert were not recognized by T2. We found that mutations in aspartic acid that did not affect the structural properties of the salt

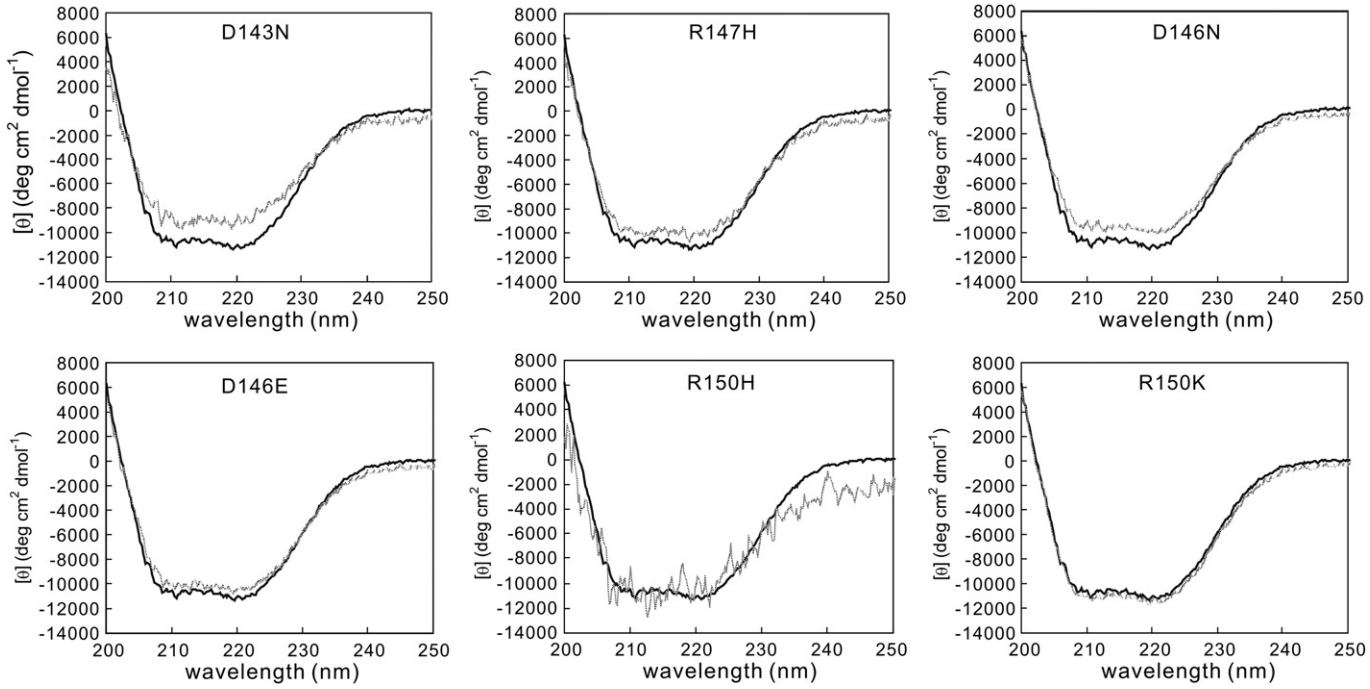

Fig. 2. Far-UV circular dichroism (CD) spectroscopy of recombinant wild type and salt bridge mutants of PrP120–230. The sample concentrations were 0.25 mg/mL except in the case of R150H (0.1 mg/mL). Samples containing wild-type PrP120–230 (solid line) and salt bridge mutants (dotted line) of PrP120–230 in PBS (pH 7.4) were scanned from 250 nm to 200 nm at 25 °C, and the resultant spectra were overlaid. Spectral minima at 222 nm and 208 nm are indicative of a high α-helical content.

bridges also did not affect the reactivity toward T2 or the ability to convert as compared to the wild-type fragment. On the other hand, when mutations in arginine affected the structure of PrP, the mutant fragments were not recognized by T2 or had lost the ability to convert.

4.2. Salt bridge mutations did not change the secondary structure of PrP

The formation of salt bridges in PrP greatly contributes to maintaining the entire structure of the protein [16,17]. Using CD, we confirmed that salt bridge mutants form secondary structures (Fig. 2). The results indicate that the salt bridge mutations did not greatly affect secondary structure formation, but the structure of neutralized-charge mutants differed from that of the wild type because of charge disruption. Secondary structure formation by deletion mutants of PrP under various external conditions has been reported [19–21]. Using CD, Speare et al. showed secondary structure formation by recombinant hamster PrP23–231, its salt bridge mutants (D144N and D147N), and a double mutant D144N/D147N [22]. They reported that all the spectra of the salt bridge mutants were completely consistent with the wild-type spectra, so they considered that mutations in the salt bridge residues do not significantly affect secondary structure formation. Moreover, they evaluated the refolding of the 3 mutant PrPs after cooling from 72.5 °C to 25 °C by CD and found that all the spectra of the 3 mutants differed from the wild-type spectra and among each other after cooling. They concluded that the reason underlying their results was that the denaturation state of the mutants at 72.5 °C differed from that of the wild type, and the reversibility of each mutant was different. They suggested that the structural properties differed between salt bridge mutants and the wild-type protein because of refolding. In our studies, the spectra of the neutralized-charge mutants were not completely consistent with the wild-type spectra. This slight difference could be related to the difference in the refolding process between the wild-type protein and the aspartic acid mutants.

4.3. Kinetic analysis of the association and dissociation of the salt bridge mutants and wild-type protein with the T2 antibody

To investigate the interaction of PrP with T2 in more detail, we kinetically analyzed the interaction by using a Biacore system (Fig. 3). The dissociation rate of the wild type was found to be very slow, and the total reaction had a high affinity. All mutants, including the salt bridge mutants, which were not detected by western blotting, bound to the T2 antibody. The association rate of the mutants was similar to that of the wild type except in the case of R150K. In contrast, the dissociation rate of the salt bridge mutants with T2 drastically differed from that of the wild type. The dissociation rate of the like-charge mutants D146E and R150K for T2 is about 10-fold faster than the dissociation rate of the wild-type fragments with T2. The dissociation rate of the neutralized-charge mutants D146N, R147H, and R150H for T2 is about 100-fold faster than the dissociation rate of the wild-type fragments with T2. The mutation in the first salt bridge (D143–R147) in the N-terminus of PrP120–230 had a negligible effect on the kinetic properties, whereas mutations in the second salt bridge (D146–R150) in the C-terminus of PrP120–230 caused substantial changes in the kinetic properties. Although the CD spectra of the like-charge mutants were consistent with the wild-type spectra, kinetic analysis showed that their dissociation rates differed. The kinetic analysis revealed differences between the mutant variants, which could not be detected spectroscopically.

4.4. The contribution of each salt bridge to the stability of helix 1 is not identical

The effect of the mutations differed among D143 at the N-terminal, salt bridge 1 and R150 at the C-terminal, and salt bridge 2 of PrP. This might be because the contribution of each salt bridge to the stability of helix 1 is not identical. Although the neutralized-charge mutant D143N had a loss of charge, its dissociation rate was nearly identical to that of the wild type. This could be because Asp143 does not contribute greatly

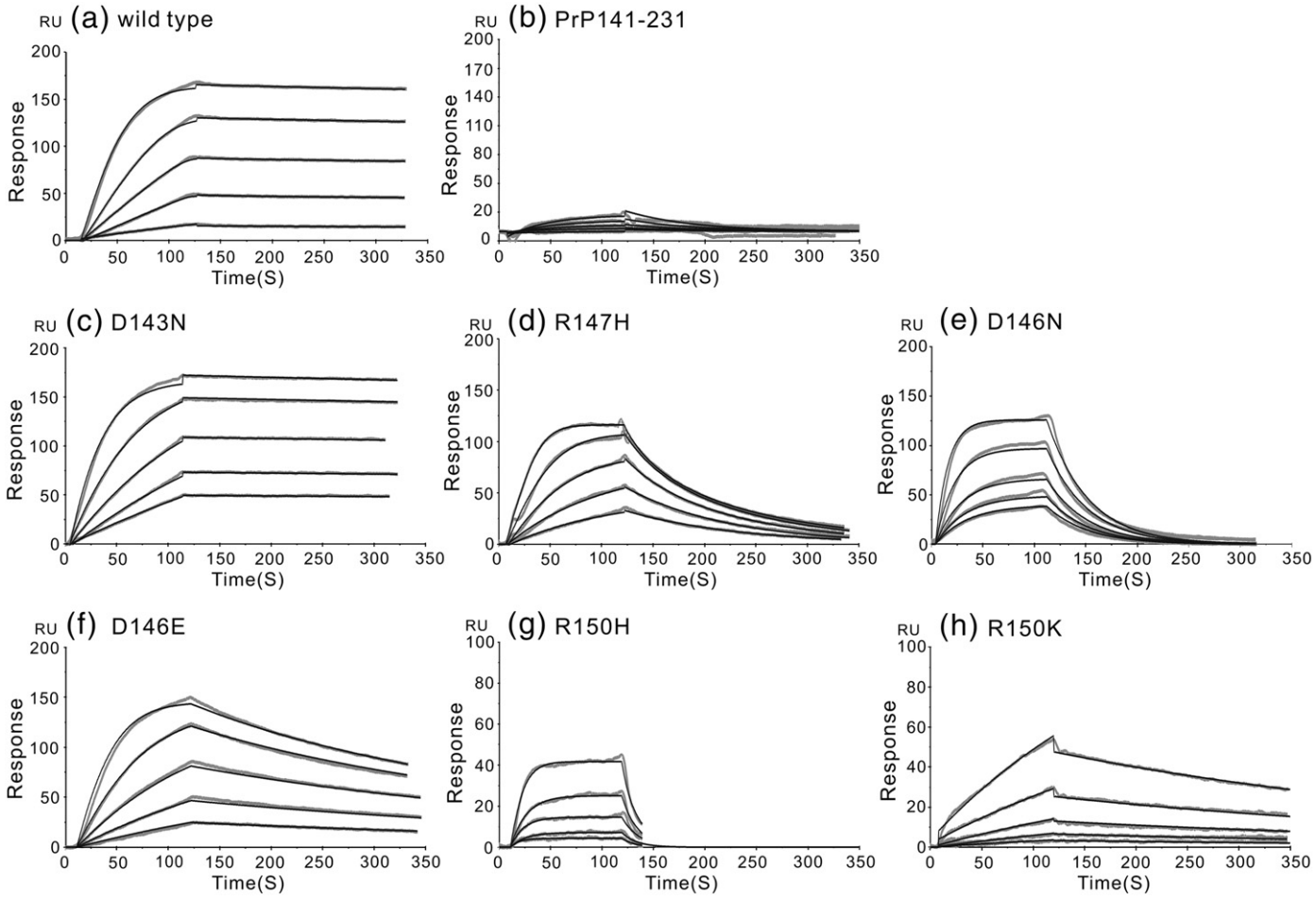

Fig. 3. Kinetic analysis of the binding of PrP recombinants to the T2 antibody by using the Biacore system. The T2 antibody was immobilized onto a CM5 sensor tip. PrP recombinants were injected over the biosensor surface twice at the indicated dilutions. The flow rate was 30 μL/min. The experimental (gray line) curves were fitted globally (black line) using the mass transfer-limiting model. (a) Wild-type PrP120–230 was injected at concentrations from 2.4 nM to 38 nM. (b) PrP141–231 was injected at concentrations from 218 nM to 3.5 μM. (c) D143N was injected at concentrations from 16.5 nM to 265 nM. (d) R147H was injected at concentrations from 50.6 nM to 809.5 nM. (e) D146N was injected at concentrations from 15.6 nM to 250 nM. (f) D146E was injected at concentrations from 3.9 nM to 62.5 nM. (g) R150H was injected at concentrations from 24 nM to 381 nM. (h) R150K was injected at concentrations from 137 nM to 2.2 μM.

to the stability of helix 1. For the like-charge mutant R150K, changes appeared not only in the dissociation rate but also in the association rate. This suggested that Arg150 is sensitive to mutation and greatly contributes to the stability of helix 1.

Norstrom and Mastrianni have reported on the relationship between mutations in the salt bridge residues and conversion of PrP^C to PrP^{Sc} [18]. They hypothesized that neutralized-charge mutants would not convert PrP^C to PrP^{Sc}, but like-charge mutants would retain the ability to convert PrP^C to PrP^{Sc}. However, they found that both neutralized-charge and like-charge D143 mutants retained the ability to convert PrP^C to PrP^{Sc} as well as the wild-type PrP fragments. Therefore, they suggested that D143 is tolerant of mutations in the amino acid residues that form salt bridges. In addition, they reported that R150 is sensitive to mutation, because both neutralized-charge and like-charge R150 mutants almost completely lost the ability to convert PrP^C to PrP^{Sc}. Our kinetic analysis results clearly indicated that mutations in the salt bridge residues changed PrP characteristics and were correlated with the ability to convert PrP^C to PrP^{Sc}, in terms of the difference in the contribution of the 2 salt bridges. It is very interesting that the reactivity pattern of PrP for T2 correlates with the conversion pattern of PrP^C to PrP^{Sc} when the salt bridges of PrP^C are mutated. This suggests the possibility that T2 can be used for PrP conversion studies.

4.5. The structural change of PrPs

For protein–protein interactions, structural changes occur with specific recognition, known as an "induced fit" [23–25]. For antigen–antibody interactions, local structural changes appear in both the antigen and antibody. Bhat et al. reported that the anti-lysozyme antibody D1.3 and its antigen change positions relative to each other on contact,

Table 1
Kinetic parameters of the interaction between the PrP recombinants and T2 calculated by Biacore. Data represent the average of three independent measurements. Wild type is PrP120–230. Abbreviations are k_a, association rate constant; k_d, dissociation rate constant; and K_D, dissociation constant.

	Wild type	PrP141–231	D143N	R147H	D146N	D146E	R150H	R150K
Charge change			−→0	+→0	−→0	−→−	+→0	+→+
k_a ($\times 10^4\ M^{-1}\ s^{-1}$)	55.63 ± 4.92	0.31 ± 0.02	16.73 ± 2.45	10.73 ± 0.21	27.06 ± 2.99	73.30 ± 1.65	8.13 ± 0.71	0.27 ± 0.02
k_d ($\times 10^{-3}\ s^{-1}$)	0.24 ± 0.02	13.57 ± 3.43	0.15 ± 0.02	11.43 ± 1.71	24.56 ± 0.51	3.37 ± 0.47	62.30 ± 2.42	2.49 ± 0.21
K_D ($\times 10^{-9}$ M)	0.44 ± 0.07	4351 ± 1024	0.91 ± 0.19	106.5 ± 15.3	91.67 ± 12.36	4.61 ± 0.69	769.0 ± 43.1	942.4 ± 35.3

whereby their bond becomes tighter [26]. The altered structure resulting from induced fit improves stability and strengthens the reaction. The structural changes in wild-type PrP are induced on its association with T2, and these changes lead to tighter binding. On the other hand, the salt bridge mutants did not show these structural changes; therefore, their dissociation was much faster and their affinity is lower. The interaction between PrP and T2 would be improved by induced fit. Without induced fit, the complexes between the salt bridge mutants and T2 would tend to dissociate more easily.

Specific antibodies are available for characterizing the novel structural properties of specific antigens. For instance, the structure of cathepsin B changes when it binds to a specific antibody, and it no longer exerts the harmful endopeptidase activity it shows in the free, non-bound form. Instead, it exerts exopeptidase activity, which is not harmful to cells [27]. Cordeiro et al. reported that PrP^C interacted with nucleic acids and some other polyanions and that this interaction drove the PrP^C to PrP^{Sc} conversion in vitro [28,29]. It is interesting to study whether the T2 antibody could inhibit PrP^C to PrP^{Sc} conversion by blocking the access of nucleic acids for PrP^C. The structural properties of proteins can be better understood by analyzing the interaction between the protein as the antigen and its specific antibody.

5. Conclusion

We studied the role of the salt bridges in PrP by investigating the mechanism by which an anti-PrP antibody, T2, recognizes salt bridge mutants. By kinetic analysis, we revealed that the salt bridges play a role mainly in the dissociation phase, not the association phase, in the interaction between PrP and T2. In addition, by kinetic analysis using the T2 antibody, we showed that the mutants, whose structural changes could not be distinguished by CD, certainly differed from wild-type PrP. These results suggest that salt bridges make the binding of T2 to PrP tighter by slowing down dissociation.

References

[1] A. Aguzzi, M. Polymenidou, Mammalian prion biology: one century of evolving concepts, Cell 116 (2004) 313–327.
[2] M.P. McKinley, D.C. Bolton, S.B. Prusiner, A protease-resistant protein is a structural component of the scrapie prion, Cell 35 (1983) 57–62.
[3] B. Oesch, D. Westaway, M. Walchli, M.P. McKinley, S.B. Kent, R. Aebersold, R.A. Barry, P. Tempst, D.B. Teplow, L.E. Hood, et al., A cellular gene encodes scrapie PrP 27–30 protein, Cell 40 (1985) 735–746.
[4] T. Kitamoto, J. Tateishi, T. Tashima, I. Takeshita, R.A. Barry, S.J. DeArmond, S.B. Prusiner, Amyloid plaques in Creutzfeldt–Jakob disease stain with prion protein antibodies, Ann. Neurol. 20 (1986) 204–208.
[5] M. Haritani, Y.I. Spencer, G.A. Wells, Hydrated autoclave pretreatment enhancement of prion protein immunoreactivity in formalin-fixed bovine spongiform encephalopathy-affected brain, Acta Neuropathol. 87 (1994) 86–90.
[6] H. Hayashi, M. Takata, Y. Iwamaru, Y. Ushiki, K.M. Kimura, Y. Tagawa, M. Shinagawa, T. Yokoyama, Effect of tissue deterioration on postmortem BSE diagnosis by immunobiochemical detection of an abnormal isoform of prion protein, J. Vet. Med. Sci. 66 (2004) 515–520.
[7] M. Enari, E. Flechsig, C. Weissmann, Scrapie prion protein accumulation by scrapie-infected neuroblastoma cells abrogated by exposure to a prion protein antibody, Proc. Natl. Acad. Sci. U. S. A. 98 (2001) 9295–9299.
[8] D. Peretz, R.A. Williamson, K. Kaneko, J. Vergara, E. Leclerc, G. Schmitt-Ulms, I.R. Mehlhorn, G. Legname, M.R. Wormald, P.M. Rudd, R.A. Dwek, D.R. Burton, S.B. Prusiner, Antibodies inhibit prion propagation and clear cell cultures of prion infectivity, Nature 412 (2001) 739–743.
[9] A.R. White, P. Enever, M. Tayebi, R. Mushens, J. Linehan, S. Brandner, D. Anstee, J. Collinge, S. Hawke, Monoclonal antibodies inhibit prion replication and delay the development of prion disease, Nature 422 (2003) 80–83.
[10] C.L. Kim, A. Karino, N. Ishiguro, M. Shinagawa, M. Sato, M. Horiuchi, Cell-surface retention of PrP^C by anti-PrP antibody prevents protease-resistant PrP formation, J. Gen. Virol. 85 (2004) 3473–3482.
[11] V. Perrier, J. Solassol, C. Crozet, Y. Frobert, C. Mourton-Gilles, J. Grassi, S. Lehmann, Anti-PrP antibodies block PrP^{Sc} replication in prion-infected cell cultures by accelerating PrP^C degradation, J. Neurochem. 89 (2004) 454–463.
[12] Y. Shimizu, Y. Kaku-Ushiki, Y. Iwamaru, T. Muramoto, T. Kitamoto, T. Yokoyama, S. Mohri, Y. Tagawa, A novel anti-prion protein monoclonal antibody and its single-chain fragment variable derivative with ability to inhibit abnormal prion protein accumulation in cultured cells, Microbiol. Immunol. 54 (2010) 112–121.
[13] E. Sasamori, S. Suzuki, M. Kato, Y. Tagawa, Y. Hanyu, Characterization of discontinuous epitope of prion protein recognized by the monoclonal antibody T2, Arch. Biochem. Biophys. 501 (2010) 232–238.
[14] R. Riek, S. Hornemann, G. Wider, M. Billeter, R. Glockshuber, K. Wuthrich, NMR structure of the mouse prion protein domain PrP(121–321), Nature 382 (1996) 180–182.
[15] L.M. Herrmann, B. Caughey, The importance of the disulfide bond in prion protein conversion, Neuroreport 9 (1998) 2457–2461.
[16] M.P. Morrissey, E.I. Shakhnovich, Evidence for the role of PrP(C) helix 1 in the hydrophilic seeding of prion aggregates, Proc. Natl. Acad. Sci. U. S. A. 96 (1999) 11293–11298.
[17] R.I. Dima, D. Thirumalai, Probing the instabilities in the dynamics of helical fragments from mouse PrP^C, Proc. Natl. Acad. Sci. U. S. A. 101 (2004) 15335–15340.
[18] E.M. Norstrom, J.A. Mastrianni, The charge structure of helix 1 in the prion protein regulates conversion to pathogenic PrP^{Sc}, J. Virol. 80 (2006) 8521–8529.
[19] L.L. Hosszu, C.R. Trevitt, S. Jones, M. Batchelor, D.J. Scott, G.S. Jackson, J. Collinge, J.P. Waltho, A.R. Clarke, Conformational properties of beta-PrP, J. Biol. Chem. 284 (2009) 21981–21990.
[20] G.S. Jackson, L.L. Hosszu, A. Power, A.F. Hill, J. Kenney, H. Saibil, C.J. Craven, J.P. Waltho, A.R. Clarke, J. Collinge, Reversible conversion of monomeric human prion protein between native and fibrilogenic conformations, Science 283 (1999) 1935–1937.
[21] K. Sasaki, J. Gaikwad, S. Hashiguchi, T. Kubota, K. Sugimura, W. Kremer, H.R. Kalbitzer, K. Akasaka, Reversible monomer–oligomer transition in human prion protein, Prion 2 (2008) 118–122.
[22] J.O. Speare, T.S. Rush III, M.E. Bloom, B. Caughey, The role of helix 1 aspartates and salt bridges in the stability and conversion of prion protein, J. Biol. Chem. 278 (2003) 12522–12529.
[23] A. Sircar, J.J. Gray, SnugDock: paratope structural optimization during antibody–antigen docking compensates for errors in antibody homology models, PLoS Comput. Biol. 6 (2010) e1000644.
[24] M. Sami, P.J. Rizkallah, S. Dunn, P. Molloy, R. Moysey, A. Vuidepot, E. Baston, P. Todorov, Y. Li, F. Gao, J.M. Boulter, B.K. Jakobsen, Crystal structures of high affinity human T-cell receptors bound to peptide major histocompatibility complex reveal native diagonal binding geometry, Protein Eng. Des. Sel. 20 (2007) 397–403.
[25] L.C. James, D.S. Tawfik, Structure and kinetics of a transient antibody binding intermediate reveal a kinetic discrimination mechanism in antigen recognition, Proc. Natl. Acad. Sci. U. S. A. 102 (2005) 12730–12735.
[26] T.N. Bhat, G.A. Bentley, G. Boulot, M.I. Greene, D. Tello, W. Dall'Acqua, H. Souchon, F.P. Schwarz, R.A. Mariuzza, R.J. Poljak, Bound water molecules and conformational stabilization help mediate an antigen–antibody association, Proc. Natl. Acad. Sci. U. S. A. 91 (1994) 1089–1093.
[27] B. Mirkovic, A. Premzl, V. Hodnik, B. Doljak, Z. Jevnikar, G. Anderluh, J. Kos, Regulation of cathepsin B activity by 2A2 monoclonal antibody, FEBS J. 276 (2009) 4739–4751.
[28] Y. Cordeiro, F. Machado, L. Juliano, M.A. Juliano, R.R. Brentani, D. Foguel, J.L. Silva, DNA converts cellular prion protein into the beta-sheet conformation and inhibits prion peptide aggregation, J. Biol. Chem. 276 (2001) 49400–49409.
[29] J.L. Silva, T.C. Vieira, M.P. Gomes, A.P. Bom, L.M. Lima, M.S. Freitas, D. Ishimaru, Y. Cordeiro, D. Foguel, Ligand binding and hydration in protein misfolding: insights from studies of prion and p53 tumor suppressor proteins, Acc. Chem. Res. 43 (2010) 271–279.